MAGNETIC RESONANCE IN CHEMISTRY, VOL. 35, 455–462 (1997)

Comparison of ^{13}C Resolution and Sensitivity of HSQC and HMQC Sequences and Application of HSQC-Based Sequences to the Total ^{1}H and ^{13}C Spectral Assignment of Clionasterol

William F. Reynolds,[1]* Stewart McLean,[1] Li-Lin Tay,[1] Margaret Yu,[1] Raul G. Enriquez,[2] Dionne M. Estwick[3] and Keith O. Pascoe[3]

[1] Department of Chemistry, University of Toronto, Toronto, Ontario, M5S 3H6, Canada

[2] Instituto de Quimica, Universidad Nacional Autonoma de Mexico, Circuito Exterior, Ciudad Universitaria, Mexico, D.F. 04510, Mexico

[3] Department of Chemistry, University of the West Indies, Mona Campus, Kingston, Jamaica

It is demonstrated that HSQC gives considerably better ^{13}C resolution and sensitivity than HMQC for CH_2 groups of natural products, particularly when combined with linear prediction. Similarly, coupled HSQC spectra provide a useful method for the determination of ^{1}H multiplet structure and consequent assignment of individual CH_2 protons as axial or equatorial in fused cyclohexane rings. These and related techniques are used to assign ^{1}H and ^{13}C spectra of the marine sterol clionasterol.

Magn. Reson. Chem. **35**, 455–462 (1997) No. of Figures: 6 No. of Tables: 1 No. of References: 22

Keywords: NMR; ^{1}H NMR; ^{13}C NMR; HSQC; HMQC; stereochemistry; clionasterol

Received 18 December 1996; revised 12 February 1997; accepted 24 February 1997

INTRODUCTION

One significant advantage of the proton-detected heteronuclear single quantum coherence experiment (HSQC)[1] over its multiple quantum analogue (HMQC)[2] is that ^{1}H–^{1}H multiplet structure appears along f_1 in the latter sequence but not in the former.[3] This should, in principle, lead to significant sensitivity and resolution advantages for HSQC over HMQC. These advantages have been clearly demonstrated for ^{1}H–^{15}N correlation experiments on macromolecules[3,4] but the advantages were much less clear for ^{1}H–^{13}C correlation experiments on macromolecules, owing to unfavourable ^{13}C T_2 relaxation characteristics with the HSQC sequence.[3] However, the latter should not be a problem for smaller natural products and one might expect to realize significant advantages for HSQC, particularly for CH_2 groups where the ^{1}H multiplets can be up to 50 Hz wide. Surprisingly, these advantages do not seem to be widely realized or appreciated, probably because ^{1}H-detected shift-correlation sequences are rarely run with sufficient ^{13}C resolution for the advantages to be obvious, reflecting the difficulty in obtaining adequate ^{13}C digitization in a reasonable time. For example, a recent review compared an HSQC and an HMQC spectrum for an alkaloid but, owing to limited f_1 data point resolution, only a small advantage was observed for HSQC.[5] However, this is not an unsurmountable problem. For many interesting natural products such as di- and triterpenes, steroids and polysaccharides, there is often severe spectral crowding in narrow ^{1}H and ^{13}C spectral regions (typically *ca.* 2–3 ppm for ^{1}H and *ca.* 50 ppm for ^{13}C) with a limited number of resolved peaks outside this region. Thus, one can obtain a low-resolution shift correlation spectrum to assign the limited number of resolved peaks combined with a higher resolution spectrom of the narrower, crowded region. The latter is aided by the availability of linear prediction methods[6] which allow one to obtain high ^{13}C resolution without having to acquire an excessive number of t_1 increment spectra.

In this paper we compare the relative resolution and sensitivity of HSQC and HMQC under high-resolution ^{13}C conditions and investigate the use of ^{13}C-coupled HSQC spectra for obtaining ^{1}H multiplet structure and HSQC-TOCSY as an aid for spectral assignments. Comparison experiments were carried out on our standard test natural product, kauradienoic acid, **1**,[7] and the HSQC sequences were used for complete spectra assignments of clionasterol, **2**, a steroid with significant spectral crowding.

RESULTS AND DISCUSSION

Comparison of HSQC and HMQC sequences and evaluation of coupled HSQC

As an initial test, we ran HSQC and HMQC spectra for the aliphatic region of **1**, using a ^{1}H spectral window of

* *Correspondence to*: W. F. Reynolds.
Contract grant sponsor: NSERCC.
Contract grant sponsor: CoNaCyT.
Contract grant sponsor: DGAPA.
Contract grant sponsor: UNAM.

 CCC 0749–1581/97/070455–08 $17.50

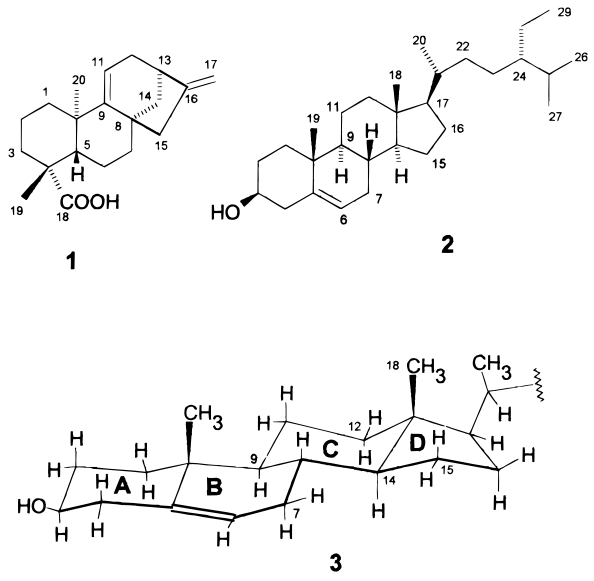

1780 Hz, a ^{13}C spectral window of 6330 Hz, 256 f_2 data points and 256 time increments. Limited f_2 resolution (*ca.* 7 Hz) was used to allow us to minimize the decoupler duty cycle. Both sets of spectra were obtained using a BIRD-nulling delay of 0.4 s (all other experimental parameters are listed in the Experimental section). Zero filling to 512 was used in f_2 while f_1 was initially zero filled to 512 and the spectra were processed without linear prediction. The data were then reprocessed, successively linearly predicting to 512 points (zero-filled to 1024), 1024 points (zero-filled to 2048) and 2048 points (zero-filled to 4096). In Fig. 1, ^{13}C contour plots are illustrated for C-6 and C-2 of **1**, chosen because H-6β and H-2α show particularly wide multiplet patterns (>40 Hz). The HSQC resolution advantages are already apparent without linear prediction (^{13}C data point resolution *ca.* 25 Hz) but are particularly dramatic for linear prediction to 2048 (^{13}C data point resolution *ca.* 3 Hz).

The sensitivity advantages of HSQC over HMQC are variable, depending upon the ^1H multiplet width and the extent of linear prediction. However, on average they are 2–3 for CH_2 groups with linear prediction to 1024, somewhat less for the narrow CH multiplets and negligible for CH_3 singlets. However, the CH_2 sensitivity is the relevant one for overall sensitivity since the CH_2 cross peaks are the weakest peaks in the HMQC spectrum. The effect upon HSQC sensitivity of the f_1 linear prediction is illustrated in Fig. 2. For each twofold increase in data points, the signal intensity approximately doubles while noise goes up by $2^{1/2}$, leading to a signal-to-noise ratio increase of *ca.* $2^{1/2}$. In fact, the enhancement on going from 256 to 2048 data points for the illustrated carbon is 300/106 = 2.83, i.e. exactly $8^{1/2}$. While the exact agreement is undoubtedly coincidental, it does illustrate the value of ^{13}C linear prediction in conjunction with HSQC. The only caveat is that there should be sufficient signal-to-noise ratio in the raw f_1 interferograms to allow for accurate linear prediction. However, this is rarely a problem with ^1H-detected sequences owing to their inherently high sensitivity. In this particular case, the ^{13}C chemical shifts determined from individual cross-sections of the highest resolution 2D HSQC spectrum agree in all cases within

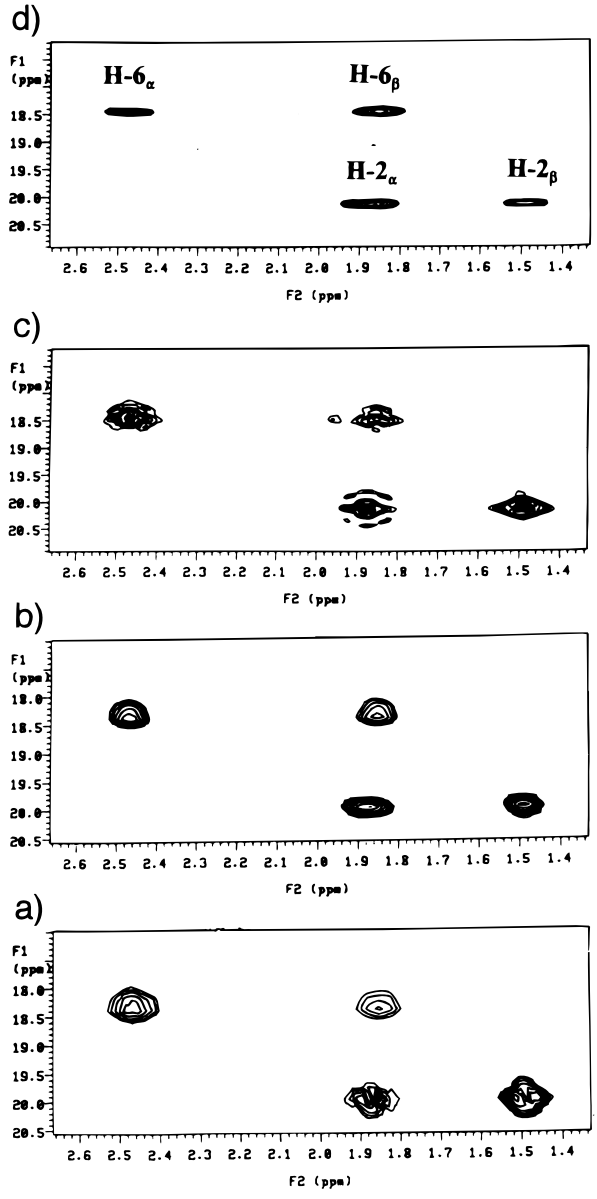

Figure 1. Contour plots for HMQC and HSQC spectra of **1** for C-2 and C-6. (a) HMQC with no linear prediction; (b) HSQC with no linear prediction; (c) HMQC linear predicted to 2048 points; (d) HSQC linear predicted to 2048 points.

0.03 ppm with those from a 1D ^{13}C spectrum, indicating that no significant errors in peak position have been introduced by the extensive linear prediction.

By contrast, the CH_2 cross-sectional spectra from the HMQC spectrum show a degradation of sensitivity with increasing linear prediction, owing to increased noise levels combined with no narrowing of f_1 linewidths. On the other hand, the CH_3 cross-sectional spectra show an increasing signal-to-noise ratio with increased linear prediction, owing to the narrowing of the singlets. This suggests a practical limitation for data point resolution, with or without linear prediction, for HMQC spectra with wide spectral windows. Specifically, there is no overall sensitivity and resolution advantage to be gained by obtaining ^{13}C data point resolution much less than the width of the widest ^1H multiplets. If improved resolution of CH_3 singlets is needed, this can still be obtained by reprocessing the data set with a

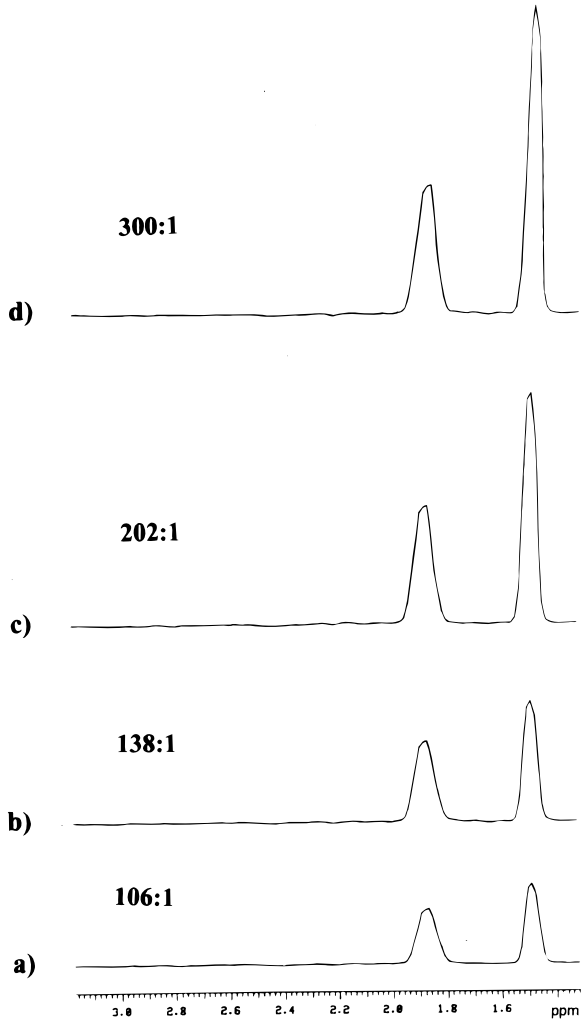

Figure 2. Cross-sections through C-2 from the HSQC spectrum of **1** with varying degrees of linear prediction. All spectra are plotted at the same absolute intensity to allow comparison of the effect of linear prediction on peak height. The measured signal-to-noise ratio is given in the upper left corner of each spectrum, with the noise measured in the high-frequency region from δ 2.8 to 3.2 where no ^1H signals are found. (a) No linear prediction (256 time increments); (b) linear predicted to 512; (c) linear predicted to 1024; (d) linear predicted to 2048.

more extensive linear prediction to yield increased ^{13}C resolution.

HSQC also allows one to obtain high resolution along both ^1H and ^{13}C axes. This is best done with no ^{13}C decoupling during acquisition to avoid problems of decoupler heating during the relatively long acquisition period necessary for excellent ^1H resolution. It has been pointed out previously that coupled HMQC can be used to determine individual ^1H multiplet patterns.[8] However, we find that the presence of ^1H multiplet structure along both axes sometimes leads to distorted cross-sections and limited ^{13}C resolution can also cause problems (see below). By contrast, HSQC suffers from neither of these problems and gives better sensitivity, an important consideration since the signal-to-noise ratio is a factor of *ca.* 2 lower relative to the ^{13}C-decoupled spectra.

We tried two versions of coupled HSQC. If the $(2J)^{-1}$ delay between the final polarization transfer and data acquisition is left in, one obtains a spectrum showing in-phase ^{13}C–^1H doublets but with small phase distortions due to evolution of ^1H–^1H coupling during the fixed delay. By contrast, a spectrum obtained with no delay between polarization transfer and data acquisition gives a spectrum with anti-phase ^{13}C–^1H doublets but no phase distortions of individual multiplets. Therefore, we prefer the latter approach. Typical ^{13}C cross-sectional spectra of **1** [obtained with 2048 data points, zero-filled to 4096 and 256 time increments, linear predicted to 1024 (with zero-filling to 2048) and with the same spectral windows as described above] are illustrated in Fig. 3. They show excellent ^1H resolution which allows one to estimate coupling constants and easily assign individual protons as axial or equatorial based on the number of large vicinal couplings.

While all of the other cross-sections show identical multiplet structures for the positive and negative peaks of each proton, this is not true for the C-6 and C-7 cross-sections (Fig. 4). In the case of C-6, the low-frequency (positive) component of each ^1H doublet is normal but the high-frequency (negative) component is distorted. The situation is the reverse for C-7 where the positive components are distorted. We suspect that this is, at least in part, a manifestation of the virtual coupling phenomenon which has been previously observed in the ^{13}C-detected HSQC sequence.[9] This occurs when a ^{13}C–^1H multiplet overlaps with a ^{12}C–^1H multiplet of an adjacent, strongly coupled proton. As noted previously,[10] this condition is fulfilled for H-7α (δ 1.975) and H-6β (δ 1.85) since the chemical shift difference (63 Hz at 500 MHz) corresponds exactly to $^1J_{CH}/2$ while $^3J_{H\text{-}6\beta,\,H\text{-}7\alpha} \approx 11$ Hz. However, although this might account for the appearance of the high-frequency H-6β multiplet and the low-frequency H-7α multiplet, this does not obviously explain the distortions noted for H-6α and H-7β since the chemical shift difference between these protons is nearly 1 ppm. The situation may be complicated because H-5β and H-6β are also close to fulfilling the virtual coupling condition (78 Hz chemical shift difference), although no distortion is noted for the C-5 multiplet patterns (not shown). Finally, the C-6 cross-section [Fig. 4(a)] shows weak ^{12}C–^1H peaks corresponding to H-5β and H-7β while that for C-7 [Fig. 4(b)] shows an H-6β peak. C-5 shows corresponding weak peaks for and H-6α and H-6β. It is uncertain whether the strong virtual coupling promotes extensive redistribution of magnetization through this strongly coupled spin system and/or whether these observations might reflect the results of minor pulse imperfections. We intend to investigate this problem further, taking advantage of the ability of SIMPLTN[11] simulate 2D spectra with both perfect and imperfect pulses.[12]

Total ^1H and ^{13}C spectral assignments for β-clionasterol with the aid of different HSQC sequences

Clionasterol [(24*S*)-24-ethylcholest-5-en-3β-ol] is the C-24 epimer of the very common plant sterol β-sitosterol.[13] These epimers are distinguished by small differences in the ^{13}C and ^1H chemical shifts of the side-chain methyl groups.[14–16] These differences allowed us

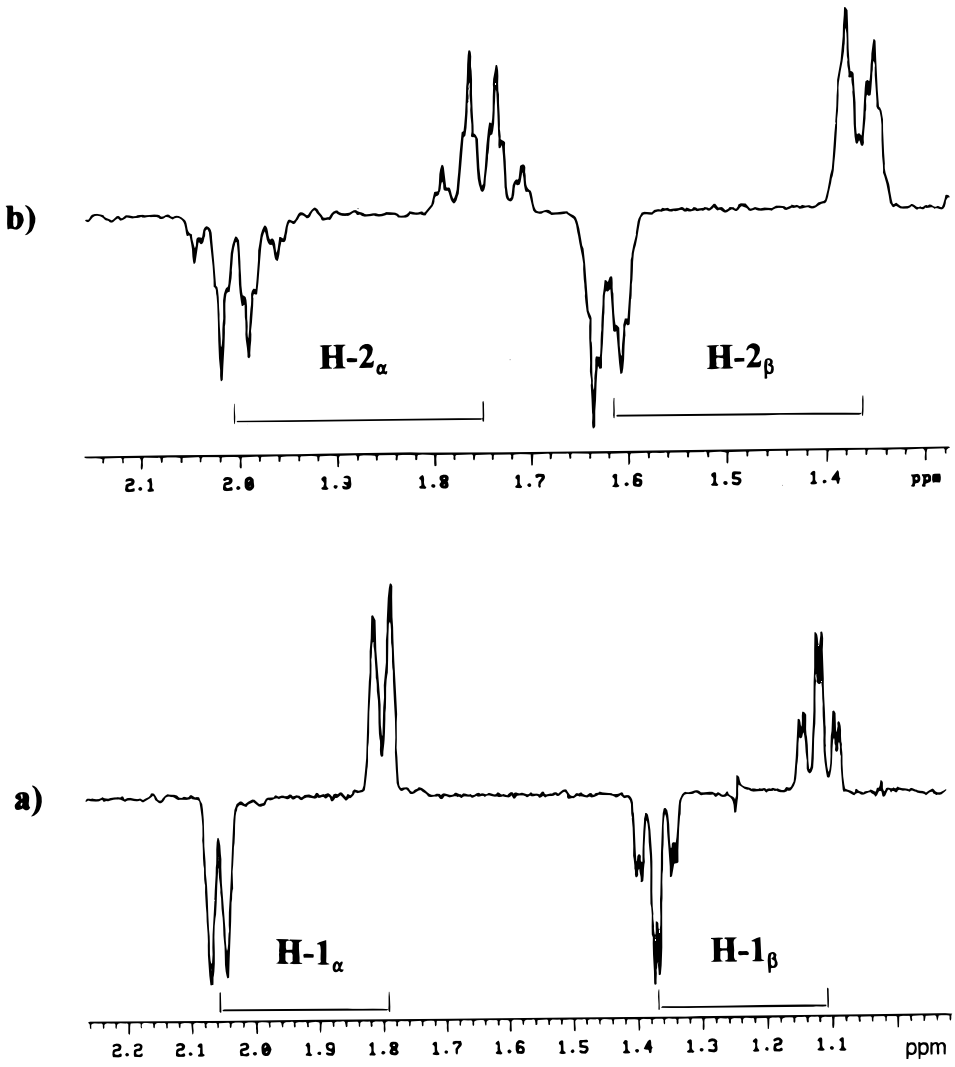

Figure 3. ^{13}C cross-sections for (a) C-1 and (b) C-2 of **1** obtained from a coupled HSQC spectrum.

to determine that the compound which we had isolated (see Experimental) was in fact clionasterol rather than sitosterol. ^{13}C chemical shifts for both sterols, along with a number of related compounds, had been assigned by empirical methods in 1978,[14] but the only assigned ^{1}H chemical shifts were the above-mentioned CH_3 assignments.[15,16] This is a relatively common situation since, for example, complete ^{1}H chemical shift assignments for cholesterol were only reported in 1996.[17] β-Clionasterol presents a challenging assignment problem since, in addition to extreme ^{1}H spectral crowding, the ^{13}C spectrum shows three protonated carbons (originally assigned as C-2, C-7 and C-8)[14] within 0.25 ppm. Consequently, we decided to carry out rigorous ^{13}C and ^{1}H chemical shift assignments for **2** in order to provide complete ^{1}H assignments. It was felt that this would provide a good test of the superior ^{13}C resolution of HSQC over HMQC, and also of the utility of related sequences such as coupled HSQC and HSQC-TOCSY.

To arrive at the assignments, normal ^{1}H and ^{13}C spectra plus a high-resolution DEPT spectrum, focusing on the aliphatic region, were run, along with COSY, HMQC, HSQC, HMBC, NOESY, coupled HSQC and HSQC-TOCSY 2D spectra.

The resolution advantages of HSQC over HMQC are particularly apparent in Fig. 5, which illustrates the one-bond ^{13}C–^{1}H peaks in the ^{13}C region δ 31.8. The HMQC spectrum shows an unresolved peak centred about δ_C 31.8/δ_H 1.5 which actually corresponds to cross peaks involving C-2, C-7 and C-8. By contrast, the HSQC spectrum shows a well resolved peak at δ_C 31.68 (δ_H 1.84, 1.50) which was assigned as C-2 based on COSY and HMBC cross peaks. However, there are two carbons at δ 31.92 and 31.93 which cannot be resolved by HSQC owing to the very small ^{13}C chemical shift difference and where two protons have relatively similar chemical shifts, centred about δ_H 1.49. Both the COSY and HSQC-TOCSY spectra suggested that the olefinic hydrogen was coupled to two hydrogens at δ 1.98 and 1.53, assignable as the C-7 methylene protons. These spectra did not allow unambiguous assignment of the chemical shift of H-8 since H-8, H-11α and H-11β, all of which have very similar chemical shifts (see Table 1), are all vicinally coupled to H-9. However, a coupled HSQC spectrum (not shown) showed distinct multiplets centred at δ 1.98, 1.53 and 1.45, allowing assignment of the latter to H-8. Finally, the assignment of C-7 and C-8 was made from a high-resolution DEPT spectrum (32 758 points for a 9000 Hz spectral window) which

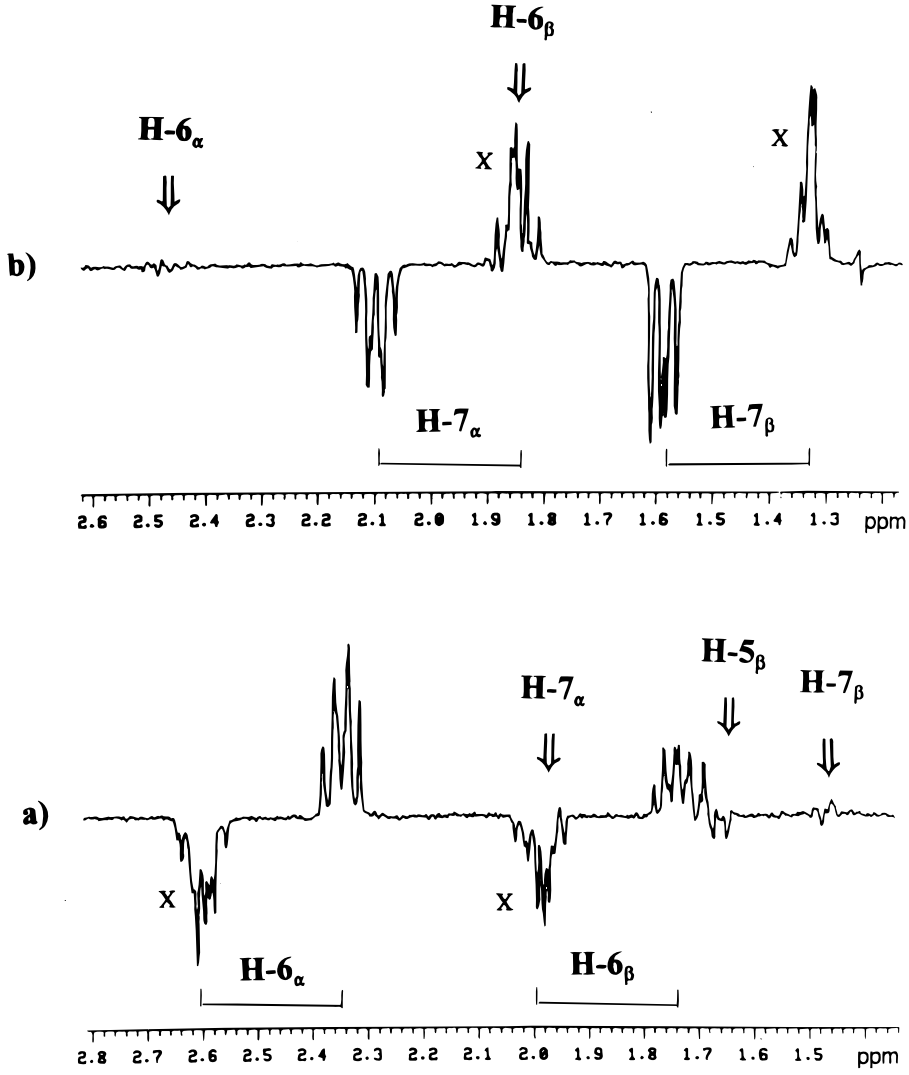

Figure 4. ^{13}C cross-sections for (a) C-6 and (b) C-7 of **1** obtained from a coupled HSQC spectrum. Multiplets which are apparently affected by virtual coupling are marked X. The chemical shifts of other coupled protons which are part of the same isolated spin system are indicated by arrows which are labelled for the protons involved.

allowed the assignment of C-7 at δ 31.93 and C-8 at δ 31.92, based on their different numbers of attached protons.

These experiments, combined with the results of an HMBC experiment, allowed completion of the basic ^{1}H and ^{13}C assignments, as listed in Table 1. ^{13}C assignments agree with the earlier empirical assignments.[14] However, the assignment of individual methylene protons as α or β proved surprisingly difficult. The expected ring conformations should be identical with those in cholesterol, as illustrated in **3**. The corresponding assignments for cholesterol in CD_3OD, based on ROESY measurements, have been reported recently.[17] Since the two molecules only differ by the attachment of the ethyl group to C-24 in **2**, we would have anticipated similar α and β assignments, allowing for small differences due to solvent effects. The NOESY spectrum which we obtained was often ambiguous, owing to severe spectral overlap. However, the cross peaks involving the β_a (the subscript a or e corresponds to an axial or equatorial orientation, respectively) methyl singlets (H-18 and H-19) were clearly observable and, in some cases, raised questions about the earlier assignments. For example, H-18 gave cross peaks with the H-15 proton at δ 1.07, suggesting that the latter proton is β_a, rather than α_e as previously suggested.[17] H-18 also shows a cross peak with the H-12 proton at δ 2.02, indicating that this proton is β_e rather than its previous assignment as α_a.[17]

The coupled HSQC spectrum allowed clear resolution of these and other uncertain assignments. For example, a cross-section through C-12 (Fig. 6) showed unambiguous ^{1}H multiplet patterns which allowed a clear assignment of the proton at δ 2.02 as β_e and the proton at δ 1.16 as α_a. This was also true for C-11 and C-15, where the current assignments (Table 1) are reversed from those made previously.[17] The only remaining ambiguity concerned C-16, where the differences in the two proton multiplet patterns were not sufficiently large to allow assignment (see Fig. 6), possibly owing to conformational flexibility in the five-membered ring. However, this was resolved with the aid of HSQC-TOCSY and HMBC experiments. The improved resolution provided by the ^{13}C axis in

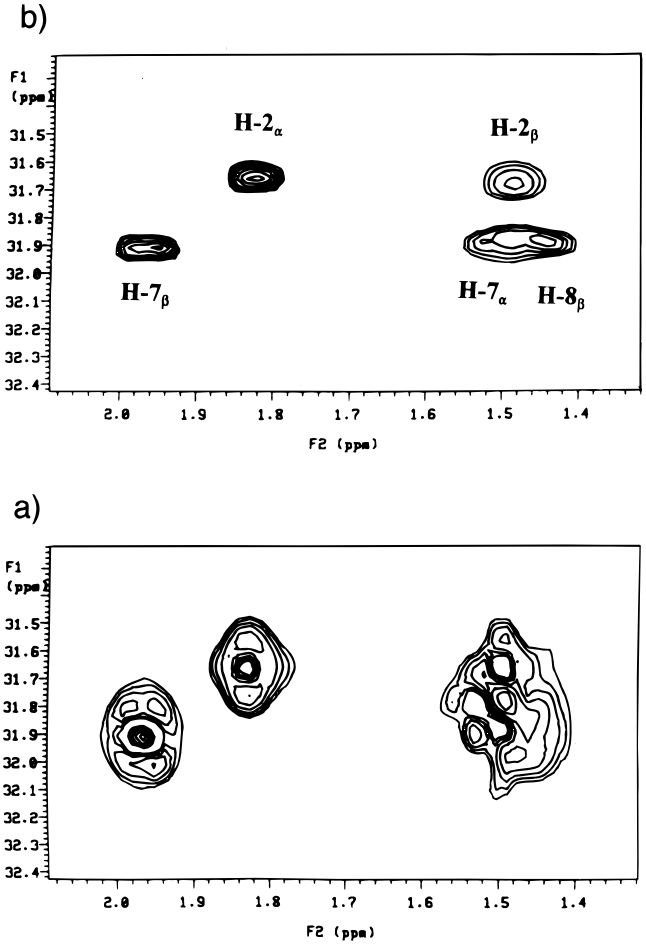

Figure 5. Contour plots for C-2, C-7 and C-8 of **2** obtained with (a) HMQC and (b) HSQC. The individual proton assignments are provided on the HSQC spectrum.

Table 1. Assigned ^{1}H and ^{13}C chemical shifts for clionasterol, 2[a]

Carbon	δ_C	δ_H α	δ_H β	Carbon	δ_C	δ_H α	δ_H β
1	37.27	1.08	1.86	16	28.25	1.84	1.27
2	31.68	1.84	1.50	17	56.08	1.11	—
3	71.84	3.52_5	—	18	11.87	—	0.68_0
4	42.31	2.24	2.29	19	19.41	—	1.01_0
5	140.76	—		20	36.28	—	1.36
6	121.72	5.35[b]		21	18.84	0.92_7	
7	31.93	1.53	1.98	22	33.92	0.98	1.36[c]
8	31.92	—	1.45	23	26.38	1.03	1.32
9	50.14	0.93	—	24	46.07	0.92	
10	36.52	—		25	28.95	1.68	
11	21.10	1.49	1.46	26	18.98[d]	0.81_2	
12	39.78	1.16	2.02	27	19.61[d]	0.83_2	
13	42.33	—		28	23.02	1.14	1.32
14	56.77	0.99	—	29	12.32	0.85_5	
15	24.32	1.58	1.07				

[a] ^{13}C and ^{1}H chemical shifts in $CDCl_3$, relative to internal $(CH_3)_4Si$.
[b] The olefinic hydrogen cannot be designated as either α or β.
[c] Side-chain methylene protons are listed in order of increasing chemical shift without designation as α or β.
[d] C-26 and C-27 are assigned as previously[14] since the spectra provide no means of distinguishing these two methyl groups.

HSQC-TOCSY minimized overlap and allowed much easier interpretation than provided by normal TOCSY spectra. ^{1}H cross-sections through C-14 were plotted with different TOCSY mixing times. H-14α showed an initial large transfer to H-15β (mixing time = 0.018 s), consistent with the large *anti* coupling between these protons. Longer mixing times (e.g. 0.05 s) showed further efficient transfer to the proton at δ 1.84, consistent with this proton being α in a pseudo-axial orientation and thus the δ 1.27 proton being β in a pseudo-equatorial environment. In addition, the δ 1.84 proton showed a strong HMBC cross peak with C-20 while the δ 1.27 proton showed a stronger cross peak with C-14 than did its geminal pair. Both of these observations are consistent with the tentative assignment given above since each of these ^{1}H–^{13}C pairs would be in an *anti*-vicinal arrangement which should have a large $^{3}J_{CH}$ coupling and consequent strong cross peak.[18]

Overall, these investigations have demonstrated the clear advantages of HSQC- and HSQC-based sequences for the assignment of natural products with severe ^{13}C and ^{1}H spectral crowding. The difficulty in carrying out these assignments (especially with respect to α and β orientations of hydrogens) probably accounts for the limited number of full ^{1}H assignments for simple steroids which have appeared in the literature. Finally, it should be noted that HMBC has ^{13}C resolution limitations dentical with those for HMQC. While this was not a major problem in this case, where the other 2D spectra provided sufficient information to overcome possible ambiguities in interpretation of the HMBC spectrum, it has been shown to be a problem in other natural products such as triterpenes.[19] However, provided sufficient sample is available, the corresponding ^{13}C-detected sequences such as COLOC[20] and FLOCK[21] are capable of providing excellent ^{13}C and ^{1}H resolution.[19] Furthermore, with modern microprobe and microtube technology, one can obtain adequate sensitivity with FLOCK in an overnight run with *ca.* 10 μmol of sample (e.g. 3 mg of **1**) and considerably less if only CH_3 cross peaks are required to complete an assignment.[22] Thus techniques are now available to solve even the most complex natural products structural and spectral assignment problems, even with relatively small sample sizes and severe spectral crowding.

EXPERIMENTAL

Isolation of 2

The green marine algae *Caulerpa sertularioides* (Chlorophyta) was collected in the shallow waters of Kingston harbour, Jamaica. The freshly harvested material was washed with water, homogenized in acetone (2 l) using a Waring blender and left standing for 24 h. The resulting suspension was filtered through a sintered-glass funnel over a bed of Celite and the acetone was evaporated on a rotary evaporator. The residue was extracted into methylene chloride (3 × 250 ml) and the organic extract dried over magnesium sulphate and evaporated to yield a dark green gum (14.50 g). The residual seaweed was dried and weighed (650 g dry weight). The crude gum (10.8 g) was chromatographed on silica gel using gradient elution with hexane–ethyl acetate of increasing polarity to provide eight fractions denoted

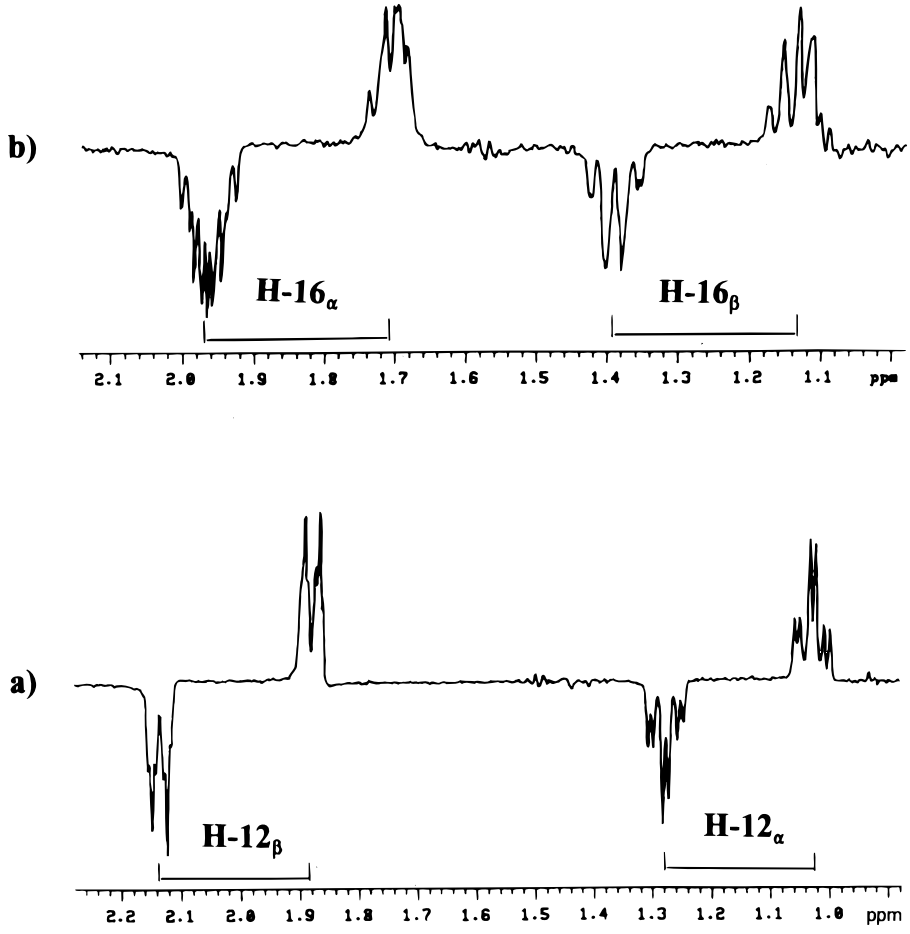

Figure 6. (a) ^{13}C cross-section for C-12 of **2**, obtained from a coupled HSQC spectrum. H-12α can be clearly recognized as an axial proton since it shows a large geminal coupling and a large *anti*-vicinal coupling to H-11β, as well as a smaller *gauche*-vicinal coupling to H-11α, while H-12β only shows a large geminal coupling and two small *gauche*-vicinal couplings. (b) ^{13}C cross-section for C-16 of **2**, obtained from the same spectrum. Note that the positive multiplet peaks show distortions similar to those in Fig. 4. This may be due to virtual coupling with H-17 at δ 1.11 since the latter ^{1}H signal overlaps with the lowest frequency H-16β multiplet.

A–H in order of increasing polarity. Fraction E was further purified by flash chromatography [hexane–ethyl acetate (80:20)] and preparative layer chromatography (chloroform) to yield crude clionasterol (174 mg). The crude material was recrystallized from acetone as needle-shaped crystals (m.p. 140–141 °C).

NMR experiments

HMQC, HSQC, HMBC, COSY and NOESY sequences were used as provided in the Varian software library. The HSQC sequence was modified to eliminate the final delay between polarization transfer and data acquisition in order to obtain ^{13}C-coupled HSQC spectra and a 90° zero frequency phase shift was applied to the data prior to Fourier transformation in order to achieve the desired absorption mode display. Alternatively, one could alter the phase of the final ^{1}H pulse by 90° relative to that for the decoupled HSQC sequence in order to obtain the same result. The HSQC-TOCSY sequence was generated by inserting the existing sequence code for HSQC in place of the HMQC segment of an HMQC-TOCSY sequence.

All spectra were obtained on a Varian UNITY-500 NMR spectrometer equipped with a 5 mm inverse detection probe (^{1}H 90° pulse width 9.5 μs and ^{13}C decoupler 90° pulse width = 9.4 μs), operating at a temperature 25 °C. Spectra were obtained with 5 mm tubes containing 8 mg of **1** dissolved in *ca.* 1 ml of $CDCl_3$ or 8 mg of **2** dissolved in *ca.* 1 ml of $CDCl_3$. Each solution contained 0.1% $(CH_3)_4Si$ as internal reference. The spectra shown in Figs 1–6 were obtained with a ^{13}C (f_1) spectral window of 6330 Hz and a ^{1}H spectral window of 1780 Hz. Decoupled HMQC and HSQC spectra were acquired in the phase-sensitive mode with 256 data points, zero filled to 512 and two sets of spectra with 256 time increments each. The relaxation delay was 1.6 s, 16 spectra were collected per time increment and ^{13}C GARP decoupling was applied during acquisition. Differing degrees of linear prediction were used, as discussed earlier, using the standard Varian linear prediction software. Gaussian weighting was applied to the raw data and to the t_1 interferograms prior to Fourier transformation. The value of the Gaussian time constant for the f_1 domain was doubled with each doubling of predicted points by linear prediction, ranging from 0.022 s for the data without linear prediction (256 points) to 0.176 s for linear prediction to 2048, to match the doubling of evolution time for the interferogram.

The coupled HSQC spectra were obtained using 2048 data points (zero-filled to 4096) with f_1 linear prediction to 1024 points (zero-filled to 2048), 32 transients per

time increment and a relaxation delay of 0.6 s. All other parameters were identical with those given above. COSY spectra and phase-sensitive NOESY spectra were obtained with equal f_1 and f_2 windows of 3125 Hz, 1024 data points and 512 time increments, linearly predicted to 1024. COSY spectra were obtained with relaxation delays of 0.8 s while the corresponding delay for NOESY was 2.0 s. The NOESY mixing time was 0.4 s while HSQC-TOCSY spectra were obtained for a series of mixing times ranging from 0.006 to 0.05 s. Low-resolution HSQC spectra, HMBC spectra and HSQC-TOCSY spectra were all obtained using 3125 Hz f_2 and 16 000 Hz f_1 spectral windows, 1024 data points and 256 time increments, linearly predicted to 2048.

Acknowledgements

Financial support from NSERCC (W.F.R. and S.McL.) and CoNaCyT and DGAPA, UNAM (R.G.E.) is gratefully acknowledged.

REFERENCES

1. G. Bodenhausen and D. J. Ruben, *Chem. Phys. Lett.* **69**, 185 (1980).
2. A. Bax and S. Subramanian, *J. Magn. Reson.* **67**, 565 (1986).
3. A. Bax, M. Ikura, L. E. Kay, D. A. Torchia and R. Tschudin, *J. Magn. Reson.* **68**, 304 (1990).
4. T. J. Norwood, J. Boyd, J. E. Heritage, N. Soffe and I. D. Campbell, *J. Magn. Reson.* **87**, 488 (1990).
5. G. E. Martin and R. C. Crouch, in *Alkaloids*, edited by H. F. Linskens and J. F. Jackson, p. 25. Springer, New York (1994).
6. C. F. Tirende and J. F. Martin, *J. Magn. Reson.* **81**, 577 (1989).
7. W. F. Reynolds, R. G. Enriquez, L. I. Escobar and X. Lozoya, *Can. J. Chem.* **62**, 2421 (1984).
8. D. Yang, X. Xu and C. Ye, *Magn. Reson. Chem.* **30**, 711 (1992).
9. G. A. Morris and K. I. Smith, *J. Magn. Reson.* **65**, 506 (1985).
10. K. A. Carpenter and W. F. Reynolds, *Magn. Reson. Chem.* **30**, 287 (1992).
11. T. Allman, A. D. Bain and J. R. Garbow, *J. Magn. Reson. A* **123**, 26 (1996).
12. A. D. Bain, I. D. Burton and W. F. Reynolds, *Prog. Nucl. Magn. Reson. Spectrosc.* **26**, 59 (1994).
13. J. R. Wiesig, N. Waespe-Sarcevic and C. Djerrassi, *J. Org. Chem.* **44**, 3374, (1979).
14. J. L. C. Wright, A. G. McInnes, S. Shimizu, D. G. Smith, J. A. Walter, D. Idler and W. Khalil, *Can. J. Chem.* **56**, 1898, (1978).
15. T. Matsumoto, T. Shizemoto and T. Itoh, *Phytochemistry* **22**, 2622 (1983).
16. C. A. N. Catalan, W. C. M. C. Kokke, C. Duque and C. Djerassi, *J. Org. Chem.* **48**, 5207 (1983).
17. P. Muhr, W. Likkusar and M. Schubert-Zsilavecz, *Magn. Reson. Chem.* **34**, 137 (1996).
18. P. E. Hansen, *Prog. Nucl. Magn. Reson. Spectrosc.* **14**, 175 (1981).
19. S. McLean, W. F. Reynolds, J.-P. Yang, H. Jacobs and L. L. Jean-Pierre, *Magn. Reson. Chem.* **32**, 422 (1992).
20. H. Kessler, C. Griesinger, J. Zarbock and H. R. Loosli, *J. Magn. Reson.* **57**, 331 (1984).
21. (a) W. F. Reynolds, S. McLean, M. Perpick-Dumont and R. G. Enriquez, *Magn. Reson. Chem.* **27**, 162 (1989); (b) K. A. Carpenter, W. F. Reynolds, J.-P. Yang and R. G. Enriquez, *Magn. Reson. Chem.* **30**, S35 (1992).
22. W. F. Reynolds, M. Yu and R. G. Enriquez, *Magn. Reson. Chem.*, in press.

